17th World Conference on Earthquake Engineering, 17WCEE
Sendai, Japan - September 13th to 18th 2020
Paper N° C001112
Registration Code: S-A02987

Floor Isolation System for Museum Contents

E. Zavala[(1)], R. Proaño[(2)], M. Torres[(3)], L. Estacio[(4)], F. Garcia[(5)]

[(1)] *Japan-Peru Center for Earthquake Engineering Research and Disaster Mitigation (CISMID-FIC-UNI), ezavalas@uni.pe*
[(2)] *Japan-Peru Center for Earthquake Engineering Research and Disaster Mitigation (CISMID-FIC-UNI), rproano@uni.edu.pe*
[(3)] *Research Institute of Civil Engineering Faculty (IIFIC-FIC-UNI), mtorres@uni.edu.pe*
[(4)] *Research Institute of Civil Engineering Faculty (IIFIC-FIC-UNI), lestaciof@uni.pe*
[(5)] *Japan-Peru Center for Earthquake Engineering Research and Disaster Mitigation (CISMID-FIC-UNI), fgarciab@uni.pe*

Abstract

Losses caused by earthquakes on the content inside buildings, such as equipment or art objects of historical value, can be irreparable. In this sense, the use of seismic isolation devices for light objects is very important, even in high-rise buildings this problem could be aggravated due to the amplification of acceleration and velocity respect to the base of the building. For this purpose, a seismic isolation device was built for slender contents manufacture by cross linear bearings. The upper platform of Base Isolator is moved by a linear guide, the friction coefficient of the linear guide is provided by rolling friction, the increasing of dynamic friction and decreasing of static friction will be activated when the earthquake protection system runs, there will be no slipping phenomenon and the positioning accuracy can reach very high. The bearing mechanism provided the simplest means of achieving a long period in the isolation system under low gravity load. The isolation system prevented rocking of the statue on top the isolated floor and substantially reduced its acceleration response in comparison to that of a conventional floor. Overturning Accelerations of content are presented, depending on the characteristics of the seismic demand used in this Work.

Keywords: Slender Contents, Rigid Blocks, Dynamic Rocking Behavior, Seismic Isolation Device.

1. Introduction

In order to properly design earthquake protection systems for nonstructural components and/or contents that are sensitive to acceleration, it is particularly important to estimate the seismic demand according to its distribution throughout the height of the building, on which the location of the content depends. For such case, we will use the method suggested by Miranda y Taghavi [1,2] in which the hypothesis states that the structure responds elastically. Therefore, in order to estimate the demands for peak acceleration and seismic performance in the contents of the building, it will be necessary to consider the type of structural system of the building, the location in height of the content and the geometrical characteristics of such. A way to protect this valuable content from damage due to vibrations or to prevent operation from stopping in case of seismic events is to locate them in isolated bases or isolated based slabs as suggested on this research. A real scale prototype that will be tested, implemented and used as the base to estimate the response through mathematical models used in the dynamic analysis. This work consists of two stages, the analytical one that involves numerical simulation for the estimation of the structural response of the device and also the prediction of the response of the balancing and/or overturning of the rigid body and the experimental one where functioning of the base isolation device is checked.

2. Mathematical models for the estimation of the dynamic response

2.1 Estimation of peak floor accelerations

The dynamic properties of buildings with many floors get closer using an equivalent continuous model, which consists on a flexural and shear cantilever beam (Figure 1). The cantilever beams are connected by an infinite number of axially rigid members that transmit horizontal forces, through which the flexural and shear cantilevers in the combined system experience the same lateral deformation. The floor masses are supposed to remain constant along the height of the building. The response of a continuous system shown on Figure 1 when it is subject to a horizontal acceleration in the base, is given by the following differential equation (see equation 5).

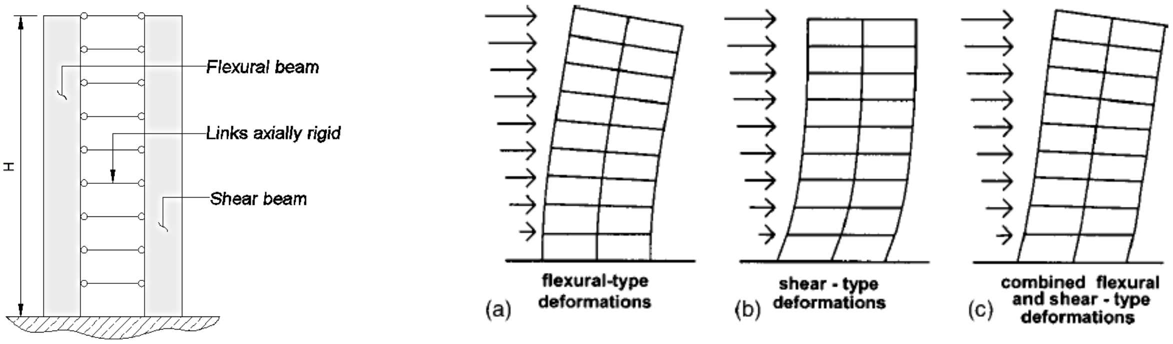

Fig. 1 – Simplified model of flexural and shear behavior [1]. Structural Systems: (a) Walls, (b) Frames and (c) Dual

$$F_i(x,t) = \frac{\rho}{EI_o}\frac{\partial^2 u(x,t)}{\partial t^2} \quad (1)$$

$$F_d(x,t) = \frac{c}{EI_o}\frac{\partial u(x,t)}{\partial t} \quad (2)$$

$$F_r(x,t) = \frac{1}{H^4}\frac{\partial^2}{\partial x^2}\left(S(x)\frac{\partial^2 u(x,t)}{\partial x^2}\right) - \frac{\alpha_o^2}{H^4}\frac{\partial}{\partial x}\left(S(x)\frac{\partial u(x,t)}{\partial x}\right) \quad (3)$$

$$F_e(x,t) = \frac{-\rho(x)}{EI_o}\frac{\partial^2 u_g(t)}{\partial t^2} \tag{4}$$

$$F_i(x,t) + F_d(x,t) + F_r(x,t) = F_e(x,t) \tag{5}$$

Where ρ(x) is equal to the mass per unit length in the model; u(x,t) is the lateral displacement at nondimensional height with respect to the total height of the building (zero at the base and one at the roof level) at time t; H is the height of the building; c(x) is the damping coefficient per unit length; EI(x) is the rigidity to flexure of a beam along its length; GA(x) is the rigidity to shear of the beam; and $u_g(t)$ is the ground displacement at time t. The variation of flexural stiffness and shear stiffness along its length can be expressed as a function of flexural rigidity and shear rigidity at the base of the structure as follows $EI(x)=EI_oS(x)$ y $GA(x)=GA_oS(x)$. Being S(x) a non dimensional function that defines the variation of the rigidity along the height of the building, the variation of the shear rigidity is supposed to be the same as the flexural rigidity; EI_o y GA_o are the flexural and shear rigidity at the base respectively. The non dimensional parameter $\alpha_o=H(GA_o/EI_o)^{0.5}$ controls the participation level of flexural and shear deformations on a simplified model of a building with multiple degrees of freedom. A value of α_o equal to zero represents a pure flexure model (Figure 1a) and a value equal to ∞ corresponds to a pure shear model (Figure 1b). An intermediate value of α_o corresponds to multistory buildings that combine shear and flexural deformations (Figure 1c). Shear wall and braced frame buildings usually have values of α_o between 0 y 1.5; buildings with dual structural systems consisting of a combination of moment-resisting frames and shear walls or a combination of moment-resisting frames and braced frames generally have values of α_o between 1.5 y 5; whereas moment-resisting frame buildings usually have values of α_o between 5 and 20 [1,2].

2.2 Principles of seismic isolation

Most isolation systems are not linear in their relationships of force-deformation, but it is not necessary to consider these non-linear effects in this introductory treatment for the objective pursued. A linear analysis would be useful for our aim to obtain information about the dynamic of the isolated base of rigid bodies. However, the non-linearity in the force-deformation relationship must be considered for the final design. For that effect, we will consider a rigid structure of a floor that will be isolated as Figure 2 shows, along with its dynamic properties, concentrated mass m, lateral stiffness k and damping coefficient c. This corresponds to a system of a degree of freedom with natural frequency ω_n, natural period T_n and damping ratio ξ. We will use the sub-index f instead of n to point out that these are properties of the structure with fixed base. As Figure 2 shows, the structure of a floor is built over the base slab m_b, which is also supported by the base isolation system with lateral stiffness k_b and linear viscous damping c_b. We can interpret T_b as the natural vibration period and ξ_b as the damping ratio of the isolation system (supposing that it is a rigid structure). In order for the base isolation to be effective in the reduction of shear forces in the structure, T_b must be larger than T_f.

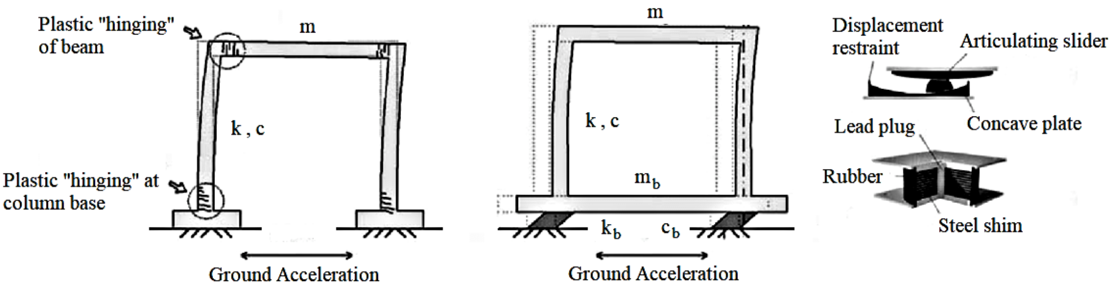

Fig. 2 – Left: Fixed structure, Right: Isolated structure [3]

$$T_f = \frac{2\pi}{\omega_f} \qquad \omega_f = \sqrt{\frac{k}{m}} \qquad \xi_f = \frac{c}{2m\omega_f} \tag{6}$$

$$T_b = \frac{2\pi}{\omega_b} \qquad \omega_b = \sqrt{\frac{k_b}{m + m_b}} \qquad \xi_b = \frac{c_b}{2(m + m_b)\omega_b} \tag{7}$$

2.3 Dynamic response of contents

The non-linear dynamic response of rigid bodies to balancing can be obtained using models available in the bibliography [4, 5, 6, 7] that solve the following equation in representation of the dynamic response of a block to balancing:

$$(I + mR^2)\ddot{\theta} = mR.\cos(\alpha - |\theta|).\ddot{y}_g - \text{sgn}(\theta).mRg.\sin(\alpha - |\theta|) \tag{8}$$

Where $\ddot{y}_g$ is the acceleration in the object base; θ is the rotation; m is the mass; I is the moment of rotational inertia; $R=(b^2+h^2)^{0.5}$ is the distance from the base border to the gravity center of the object; $\alpha=\tan^{-1}(b/h)$ is the slenderness; g is the acceleration due to gravity and sgn(.) is the Sign function. Values of 2b and 2h, the width and the height respectively of a rectangular block equivalent to non-symmetric geometry of the content on its slenderest side are shown on Figure 3. The body will start balancing when the intensity limit is reached $\ddot{y}_b=g(b/h)$ obtained at the moment of balance on the vertex in contact with the surface, ($\ddot{y}_g > \ddot{y}_b$), which only depends on the geometry of the content [8].

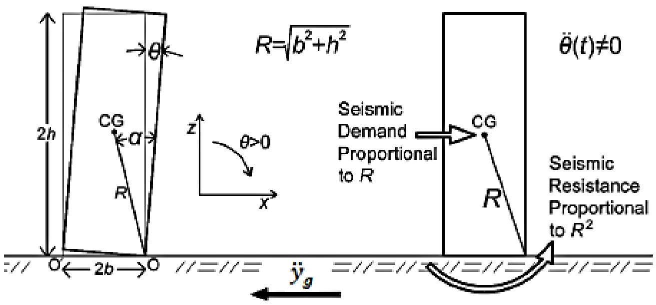

Fig. 3 – Characterization of the artistic object [9]

3. Seismic Isolation Device

It is composed by two headers with assembled rolling bearings between two linear orthogonal rails (crossed). The rolling bearings in linear configuration have a very low friction coefficient that originate negligible shear forces. In addition to these mechanical components, linear springs are included, which are the ones that provide restitution and auto-centering forces to the superior platform of the isolator. Figures 4 and 5 show the base seismic isolation device which is composed by the components described on Table 1.

Table 1 – Characteristics of the seismic isolation device

Dimensions of the Upper Base (BS) and Lower Base (BI)	60mm x 600mm
Height between the Lower base (BI) and Upper Base (BS)	47 mm
Weight (BI+BS+Mechanical Elements)	18 kgf
Number of springs / Number of rails	16 u / 8 u

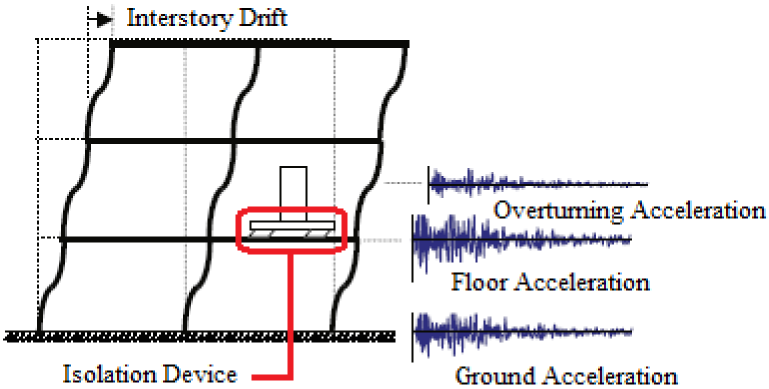

Seismic Isolator composed of linear rails TRC15

Fig. 4 – Building of fixed base with floor isolation

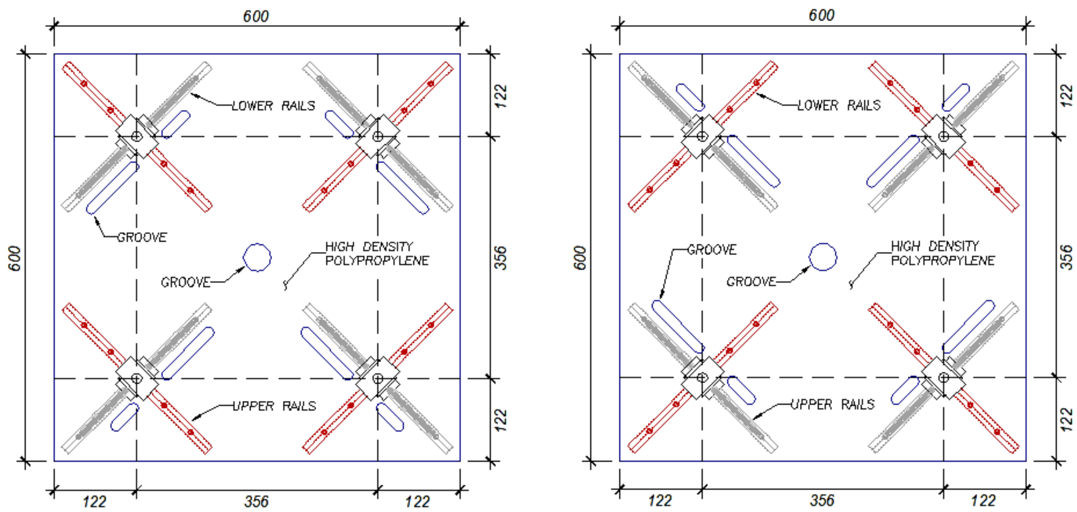

Upper Base (BS) | Lower Base (BI)

Fig. 5 – Components of seismic isolation device

In order to estimate the value of ξ_b of the system, 6 tests were carried out, 4 out of which were performed in their orthogonal directions (2 tests for each direction) and the 2 remaining, 45º in respect to their orthogonal axes. Figure 6 (left) shows two of the experimental reproductions (1-E y 2-E) corresponding to one of the orthogonal directions of the device and Figure 6 (right), the Fourier amplitude spectrum of such. On Table 2, ratios for damping are shown, measured for each direction of analysis as well as the vibration period and lateral stiffness for directions 0º, 45º and 90º.

Table 2 – Dynamic properties obtained from tests (kgf/cm)

Direction	Average		
	ξ_b (%)	T_b (s)	k_b (kgf/cm)
0º and 90º	13.33	1.43	0.548
45º	16.68	1.33	0.633

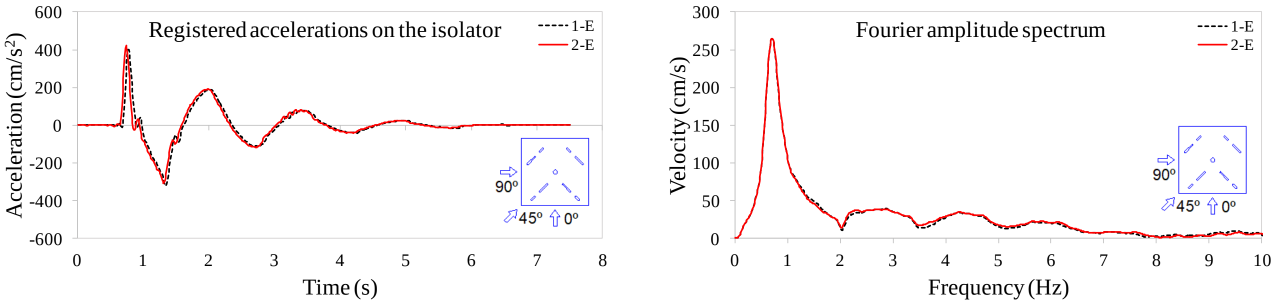

Fig. 6 – Free damped vibration (left), Transfer function (right)

4. Seismic Behavior of Contents

With the aim of performing experimental tests, a prismatic block was built, rigidized on its perimetral faces as shown on Figure 7. This wood block was put together through cubes of 30 cm x 30cm x 30cm with the purpose of carrying out a series of tests for blocks with different heights and with internal devices to add extra weight in order to modify its mass center. Table 3 states the dimensions of one of the blocks to test. The value chosen for depth was the same as the width of the block, to avoid possible torsional effects. It is important to point out that on the support surface of the block, a neoprene sheet is embedded, in order to assure the balancing and/or overturning of the block, and to avoid sliding of the rigid body on a shake table.

Table 3 – Characteristics of test specimen

Dimensions in plant / Height of the block	300mm x 300mm / 1200 mm
Weight of empty block / Weight of sand	17.8 kgf / 15 kgf
Number of cubes of 30cm x 30cm x 30cm	4 units

5. Experimental Tests on Shake Table

During the development of the seismic isolation device, there were different electronic tools with easy operation. In order to measure and collect data from tests performed, the following equipment was used: accelerographs, an Arduino UNO plate, a network adapter for schedule synchronization of the measurement equipment, an MPU6050 sensor (gyroscope) and a video camera.

For this report, only 3 tests are presented, the rest will be part of future activities and their experimental information is currently being processed. Table 4 shows different types of tests performed during experimental tests, with the aim of evaluating the dynamic behavior of the isolation device (see Figure 4) and the rigid block described on Table 3 (see Figure 7). In addition to this, the necessary instrumentation for each test and the input and output signals for each tested element are listed.

Table 4 – Measurement program for the seismic isolator and rigid block

Element	Instrumentation	Test	Input	Output
Seismic Isolator	2 Accelerometers	A	E01 Signal (accelerations on the lower base of the isolator)	S01 Signal (accelerations on the upper base of the isolator)
Rigid Block	Accelerometer + MPU6050	B1	E02 Signal (accelerations on the inferior base of the block)	S02 Signal (turning angle respect to the vertical axle of the block)
Rigid Block	Video Camara	B2	E03 Signal (photograms by Second-point of monitoring 05)	S03 Signal (photograms by Second-points of monitoring 01@04)

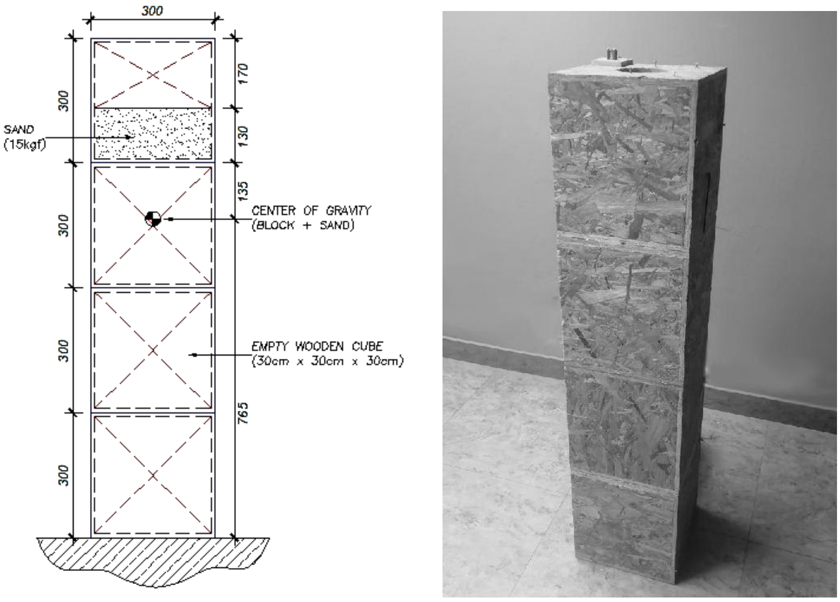

Fig. 7 – Rigid block (300mm x 300mm x 1200mm)

Table 5 – Input signals of the isolation device and the rigid block

Input Data	**Signal**	**PGA (cm/s^2)**	**PGV (cm/s)**	**PGD (cm)**	**T_p (s)**
Accelerometer 01	E01	847.60	58.63	8.17	0.39
Accelerometer 01	E02	955.50	59.18	8.56	0.59
Monitoring Point 05	E03	1196.52	82.16	8.59	0.30

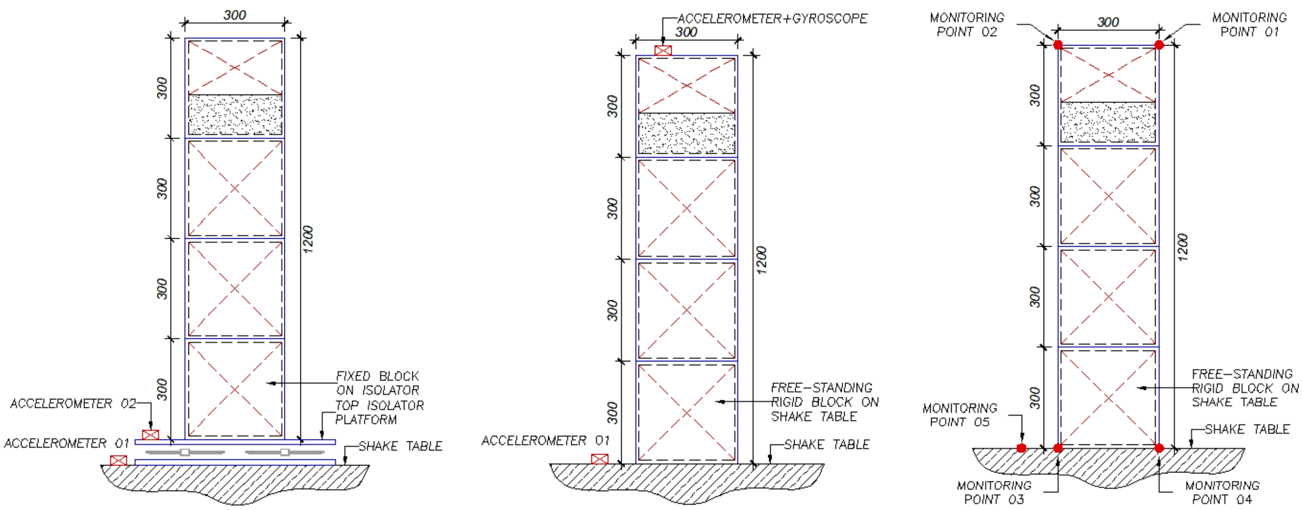

Fig. 8 – (a) Seismic isolator on shake table (b) Test specimen on shake table, accelerometers and plate MPU6050 and (c) Test specimen on shake table and video camera

5.1 Experimental Dynamic Behavior of the Seismic Isolator (Test A)

Table 5 states some parameters for the input signal E01 (PGA, PGV, PGD and predominant period associated with peak Fourier amplitude spectrum), specifically used as an excitation force at the base of the isolation device. For this test, the block described on Table 3 was used as mass, which also held on the upper platform of the isolator, in order to avoid balancing and sliding of such. The following is the isolator response (accelerometer 02, signal S01), obtained from E01 signal registered by the accelerometer 01 (see Figure 8a). On Figure 9, it can be observed that the peak registered acceleration is 120.41 cm/s^2, which is equivalent to approximately 14% of the PGA value registered by the accelerometer 01. This difference of accelerations is very noticeable because the vibration period of the isolator is much greater compared with the predominant period of E01 signal.

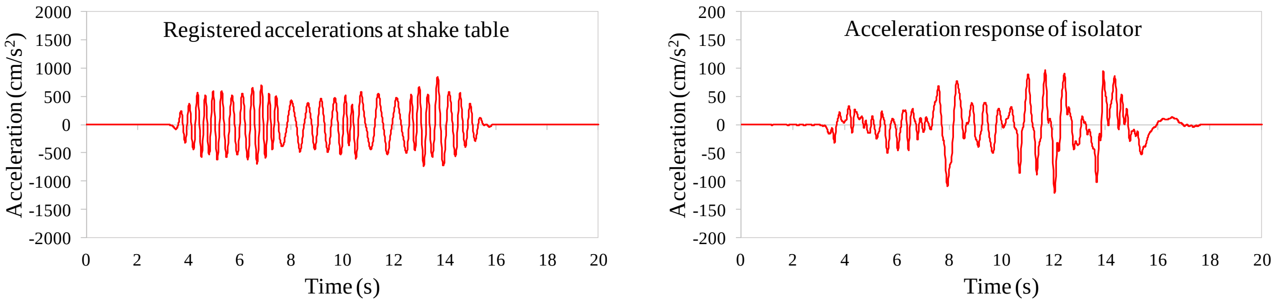

Fig. 9 – Accelerations of input signal E01, registered with accelerometer (left). Acceleration response of the isolator, registered by accelerometer 02, signal S01(right).

5.2 Experimental Dynamic Behavior of the Content (Test B)

On this section, we will study the response of rigid bodies that experienced aleatory movements. On Table 5, some parameters of input signal E02 (see figure 10) are indicated, specifically used as an excitation force in the block base described on Table 3.

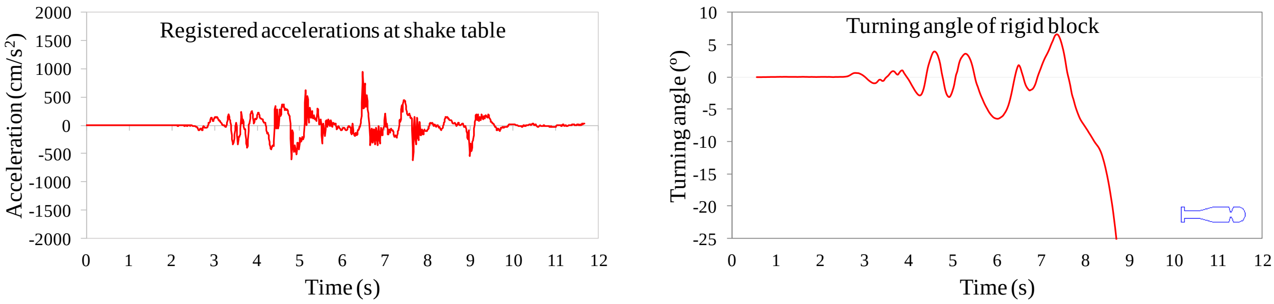

Fig. 10 – Accelerations of input signal E02, registered with accelerometer (left). Response from the turning angle in respect to the vertical axis of the block, registered by the MPU6050 sensor, S02 signal (right).

Another way of estimating the turning angles in rigid bodies is through a digital video system (photogrammetry), which registers a certain number of images per second and through a software specialized in image processing, it allows to estimate values of horizontal and vertical displacements in respect to a reference system, this was done by marking with a color on certain strategic areas (vertexes) on the block, and when processing the video, filtering the range of colors corresponding to the monitoring points on figure 8c.

With these horizontal and vertical displacements, it was possible to estimate the accelerations on the shake table and the rotations on any of the 4 vertexes of the rigid block.

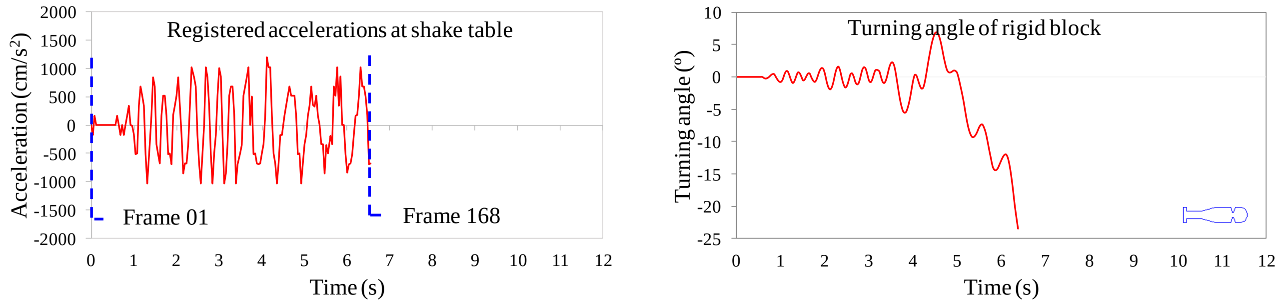

Fig. 11 – Accelerations of E03 input signal, registered with a video camera (left). Response from the turning angle in respect to the vertical axis of the block, registered with a video camera, S03 signal (right).

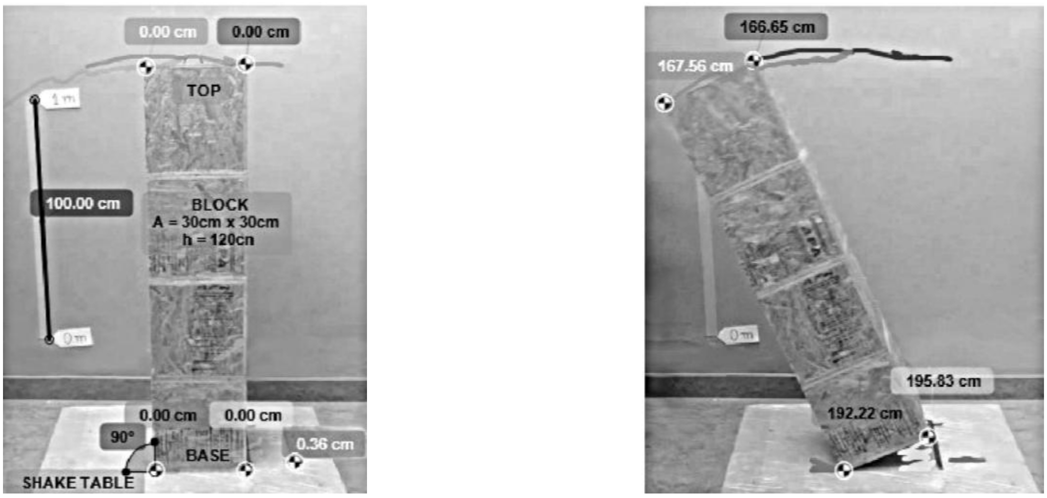

Fig. 12 – Left: Photogram 01 (beginning of the movement); Right: Photogram168 (failure limit)

5.3 Validation of results

The comparison between analytical and experimental results is presented for the three tests performed (A, B1 y B2), which have been the base for this research work. On figures 13 and 14, the non-continuous lines represent the analytical responses obtained with the equations on section 2. As you can see, the results obtained give validity to the mathematical models used in this work.

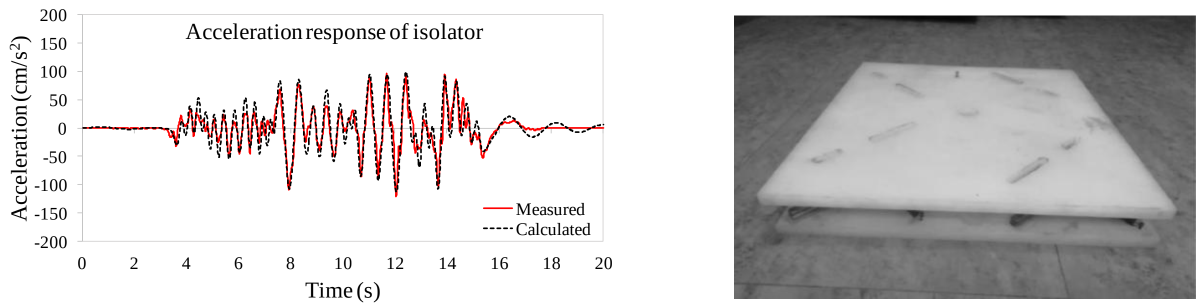

Fig. 13 – Analytical and experimental result for the base isolator (Test A)

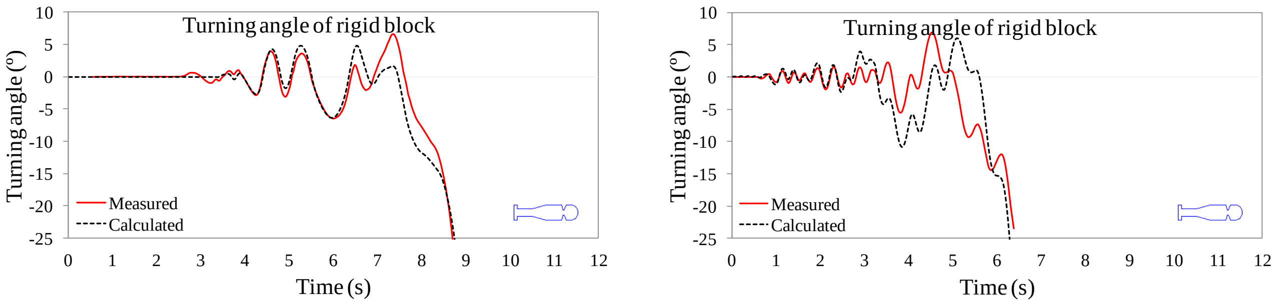

Fig. 14 – Analytical-experimental result for the rigid block, Left: Test B1, Right: Test B2

6. Contents located inside the buildings

6.1 Characteristics of the building and the content

Table 6 shows the characteristics of the building and the content in study for a subsequent simulation of dynamic behavior for both components (structural and nonstructural). Even though the contents can respond dynamically in different ways, the balancing and probable overturning ends up being one of the least wanted and riskiest modes, affecting them partially or completely.

Table 6 – Characteristics of the Building and the Content

Parameter	**Description**
Structural System / Configuration	Shear walls (α_o=1) / Regular in plant and height
Mass per unit length	1.25 tonnef.s^2/m^2
Fundamental period	1.4 s
Damping ratio	5%
Total Height / Number of Floors	84 m / 28 Levels
Dimensions of the Content / Weight of the Content	Base = 30 cm; Height = 70cm / 90 kgf

6.2 Seismic record used in the simulation

It is particularly interesting to study the effect caused by the different earthquakes about the response of buildings and, therefore, in their contents, due to the fact that the characterization of movements in the base and the dynamic properties of the building are a determining factor to predict the behavior of nonstructural components. Figure 15 illustrates the record of accelerations and the elastic acceleration spectrum for the Northridge 1994 earthquake, calculated with a damping ratio of 5%.

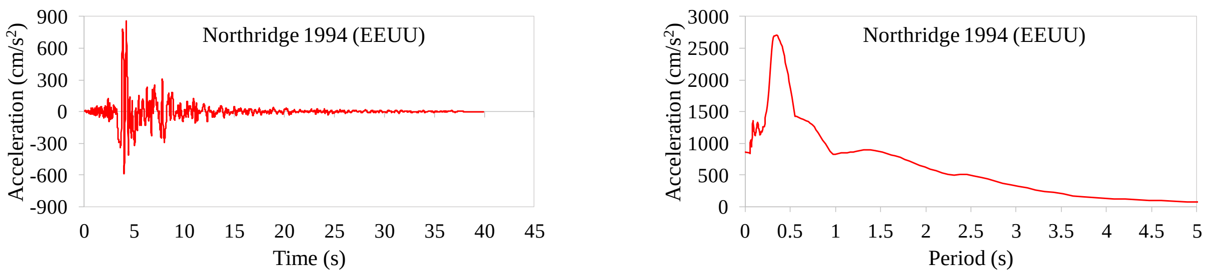

Fig. 15 – Northridge 1994 Earthquake, Record of Accelerations (left), Elastic Spectrum, 5% (right)

6.3 Dynamic response of the content

Figure 16 shows the distribution of accelerations in height of the building. For the evaluation of floor accelerations, we have considered mass and rigidity distribution uniform in height, a linear elastic behavior of the building and the same damping value for all modes considered. Figure 17 shows the response of a prismatic rigid body for a vibration mode that implies balancing and/or overturning, and it is obtained through a nonlinear formulation that describes movement of a body in respect to its mass center, in function to the acceleration history on its base, mass, moment of inertia and geographic dimensions.

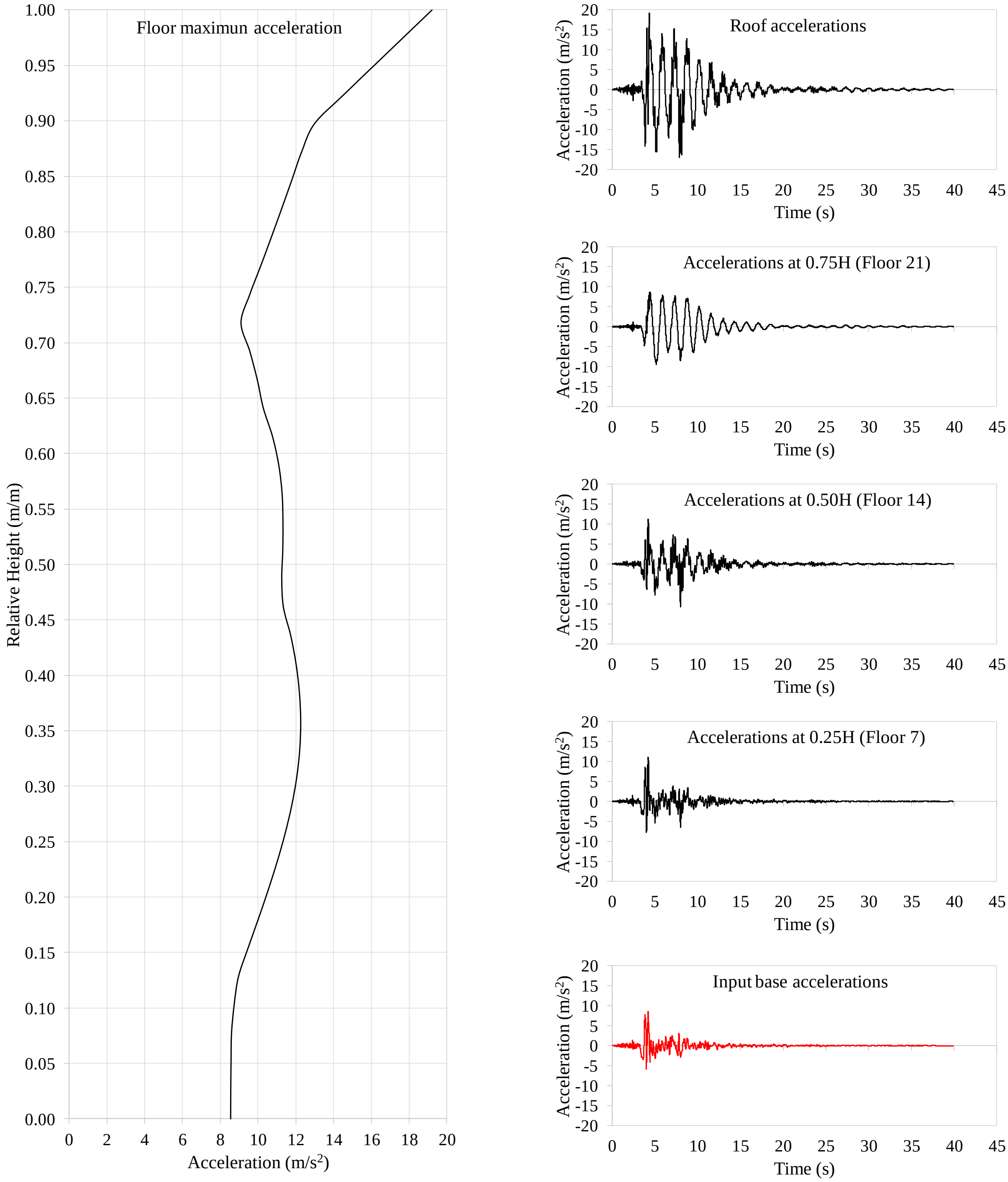

Fig. 16 – Floor accelerations for the building of shear walls of 28 levels (Northridge 1994 Earthquake)

From this figure, it can be clearly observed that there is not a defined pattern for the behavior of an object inside a building, but it can be associated with the relationship existing between peak intensities of movement at the level it is located. On Figure 16, a noticeable increase in acceleration pulses can be observed in height, so the object loses stability falling over the upper levels of the building.

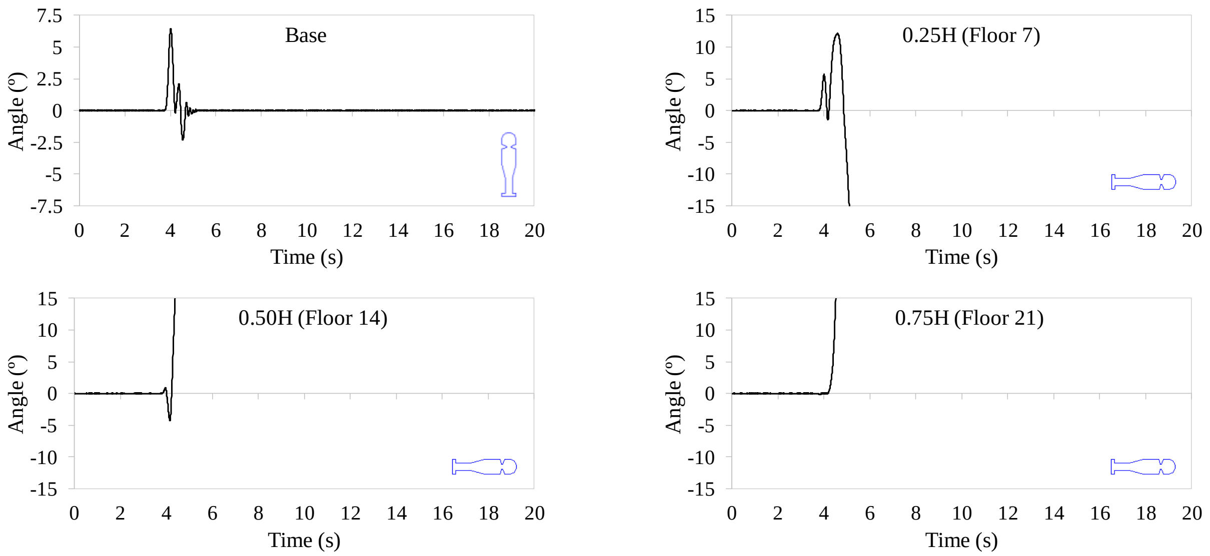

Fig. 17 – Influence of the dynamic response of the block of 30cm x 160cm due to the increase in height of the building affected by the Northridge 1994 earthquake

7. Acknowledgments

This work has been developed thanks to the support of the Research Institute of the Faculty of Civil Engineering (IIFIC) of the National University of Engineering. The results of this work are dedicated to those people who, in one way or another, made it possible to complete this project.

8. References

[1] Taghavi S, Miranda E (2005): Approximate floor acceleration demands in multistorybuildings. *Journal of Structural Engineering*, USA.

[2] Taghavi S, Miranda E (2003): Response assessment of nonstructural building elements. *Pacific Earthquake Engineering Research Center*. California, USA.

[3] Yaghmaei S, Safari S, Abdolmohammad K (2017): Characterization of ductility and inelastic displacement demand in base-isolated structures considering cyclic degradation. *Journal of Earthquake Engineering*, USA

[4] Housner G (1963): The behavior of the inverted pendulum structures during earthquakes. *Bulletin of the Seismological Society of America*, USA.

[5] Ishiyama Y (1984): Motions of rigid bodies and criteria for overturning by earthquake excitations. *New Zealand National Society for Earthquake Engineering*, New Zealand.

[6] Makris N, Roussos Y (2000): Rocking response of rigid blocks under near-source ground motions. *Geotechnique 50*, California, USA.

[7] Shenton H, Jones N (1991): Base excitation of rigid bodies. *Journal of Engineering Mechanics*, USA.

[8] Milne J (1985): Seismic experiments. *Transactions of the Seismological Society of Japan*, Japan.

[9] Makris N (2018): The dynamics of rocking Isolation. *University of Central Florida*, Orlando, USA.